Supporting Information

Enhancing anionic redox stability by oxygen coordination configurations

Haoxin Li[abc], Yining Li[bc], Xiaolin Zhao[bc], Yang Gan[bc], Wujie Qiu[bc] and Jianjun Liu*[abc]*

[a]School of Chemistry and Materials Science, Hangzhou Institute for Advanced Study, University of Chinese Academy of Science, 1 Sub-lane Xiangshan, Hangzhou, 310024, China

[b]State Key Laboratory of High Performance Ceramics and Superfine Microstructure, Shanghai Institute of Ceramics, Chinese Academy of Sciences, 1295 Dingxi Road, Shanghai 200050, China

[c]Center of Materials Science and Optoelectronics Engineering, University of Chinese Academy of Sciences, Beijing 100049, China

*Email: jliu@mail.sic.ac.cn; wjqiu@mail.sic.ac.cn

Supplementary Figures

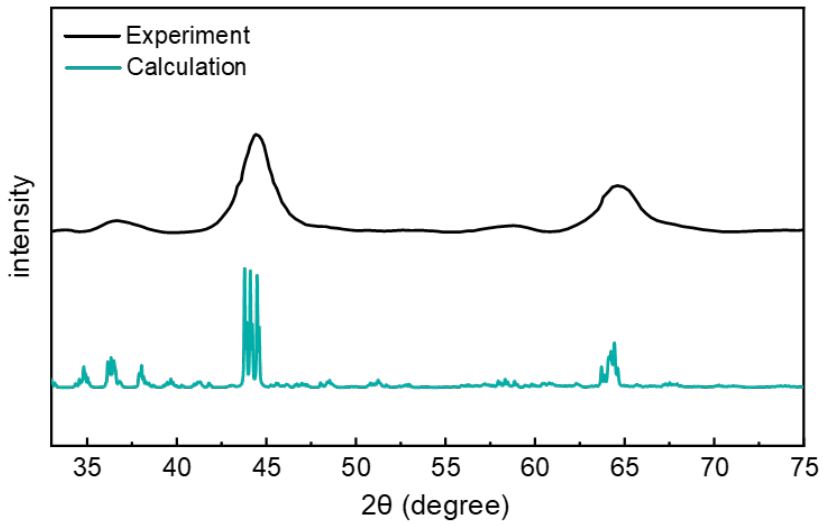

Fig. S1 The XRD spectrum of the stable structure (Fig. 1c).

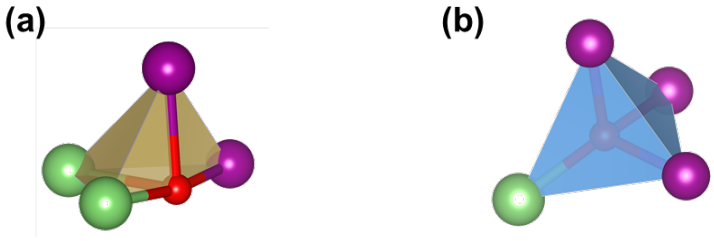

Fig. S2 Two four-coordinated oxygen configurations. (a) Oxygen is located at the edge of the tetrahedron (Oct-4); (b) Oxygen is located at the center of the tetrahedron (Tet-4).

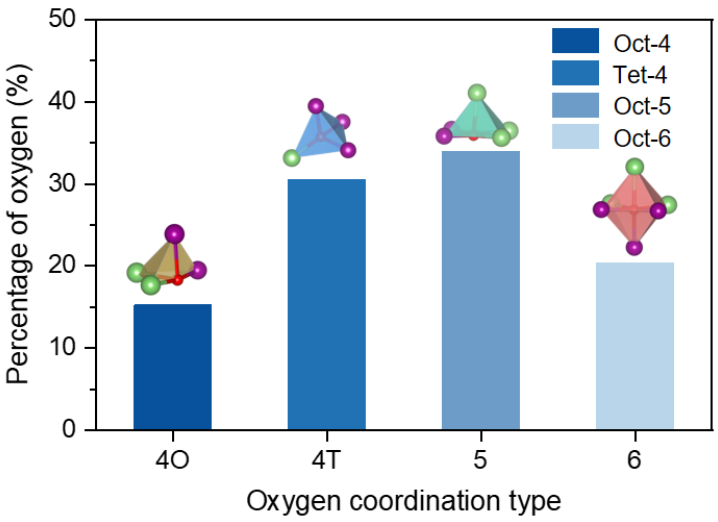

Fig. S3 The distribution of the four types of oxygen coordination configurations in $L_{1.7}Mn_{1.7}O_{3.7}F_{0.3}$.

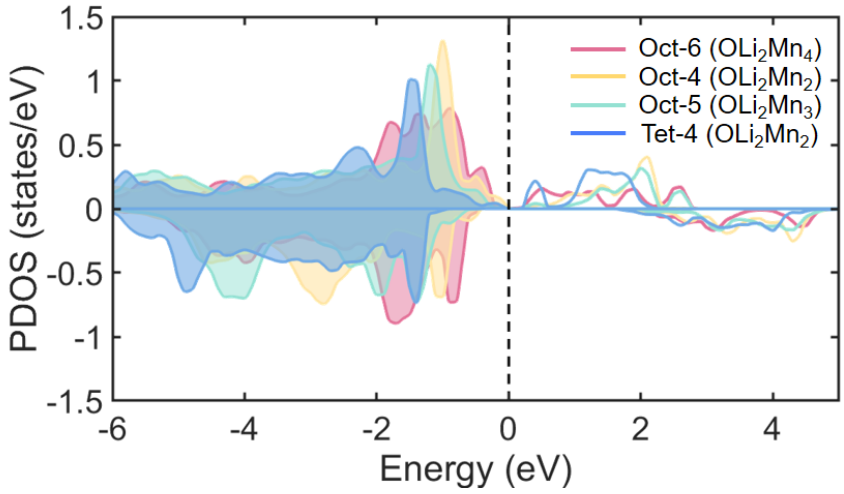

Fig. S4 Electronic structural characterization of local configurations of $OLi_2Mn_{(x-2)}$ among four oxygen coordination configurations, where x = 4, 5, 6.

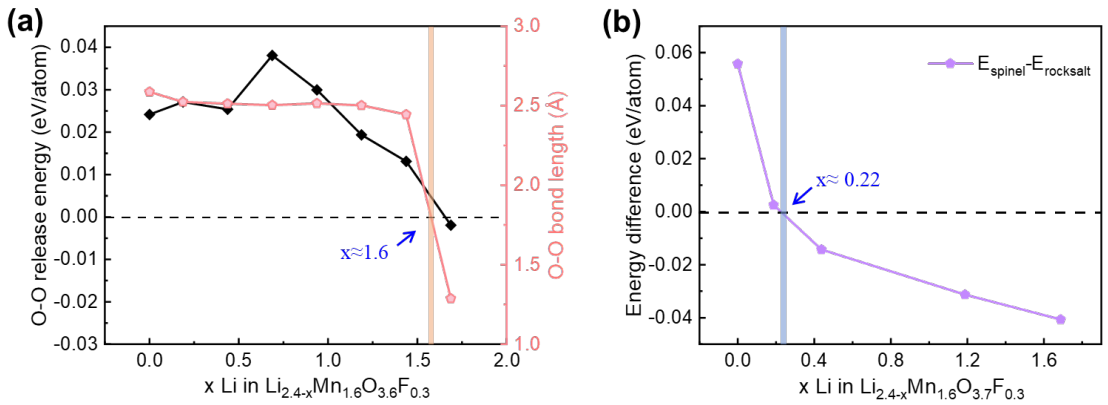

Fig. S5 Reversible boundaries for charging and discharging of $L_{2.4}Mn_{1.7}O_{3.7}F_{0.3}$. (a) Oxygen vacancy energy and the minimum O-O bond length define the reversible boundary of charging, and $x \approx 1.6$ is the boundary. (b) The energy difference between the spinel structure and the rock salt structure of the same chemical formula defines the reversible limit of discharge, and $x \approx 0.22$ is the boundary.

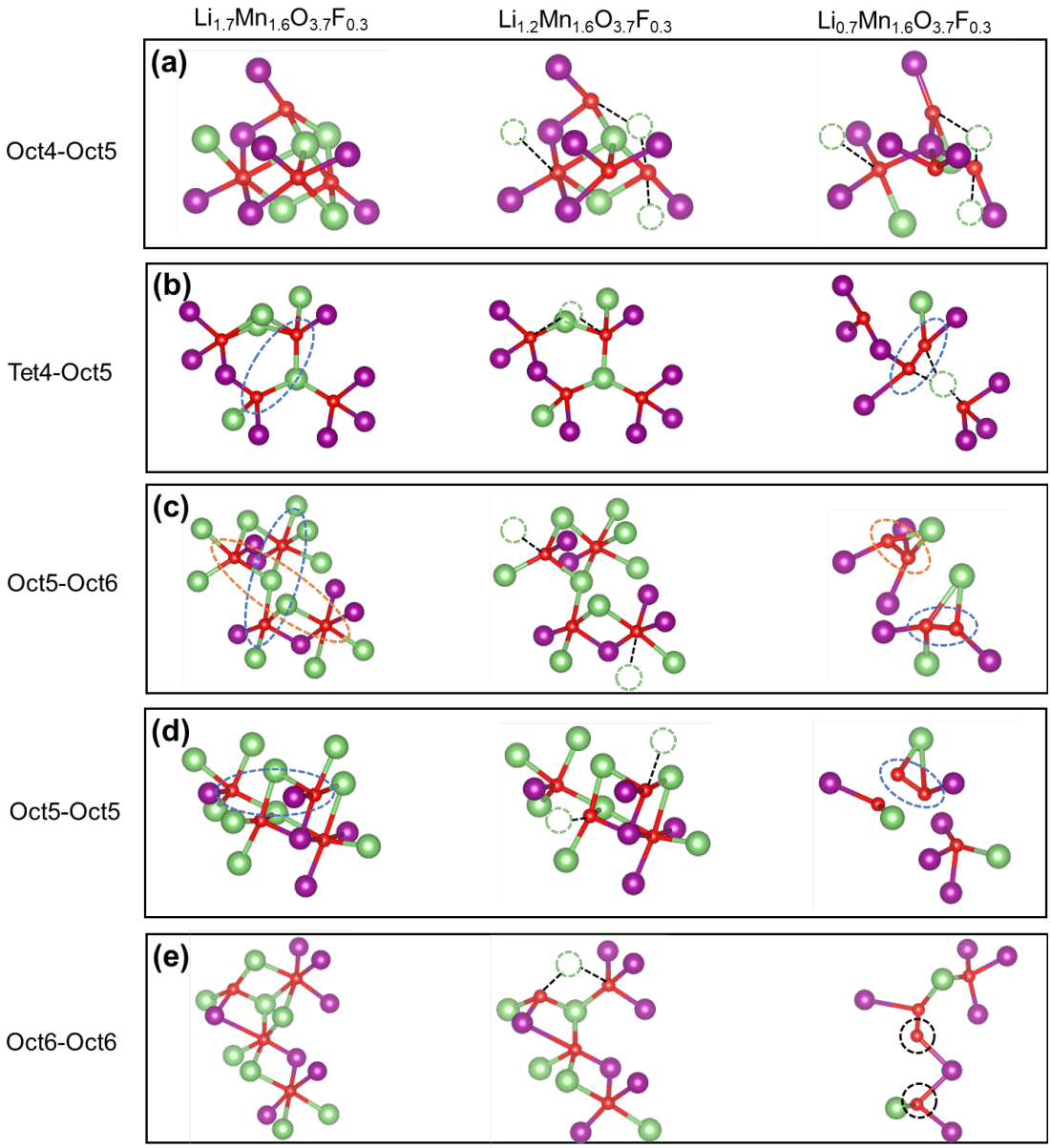

Fig. S6 Illustration of the local structural evolution of various O-O coordination configurations in $Li_{1.7}Mn_{1.6}O_{3.7}F_{0.3}$. Atomic configurations of fully lithiated and partially delithiated excess materials in $Li_{1.7}Mn_{1.6}O_{3.7}F_{0.3}$, $Li_{1.2}Mn_{1.6}O_{3.7}F_{0.3}$, and $Li_{0.7}Mn_{1.6}O_{3.7}F_{0.3}$. (a) Oct4-Oct5 is an abbreviation for O(Oct-4)-O(Oct-5); (b) O(Tet-4)-O(Oct-5); (c) O(Oct-5)-O(Oct-6); (d) O(Oct-5)-O(Oct-5); (e) 6O-6O, the black dotted circle represents the two oxygen atoms coordinated as 6O; To simplify the presentation, not all removed lithium vacancies are plotted. Green dashed circles represent lithium ions that have been extracted during delithiation. The elliptical dotted circle represents the two oxygen atoms forming the O-O bond.

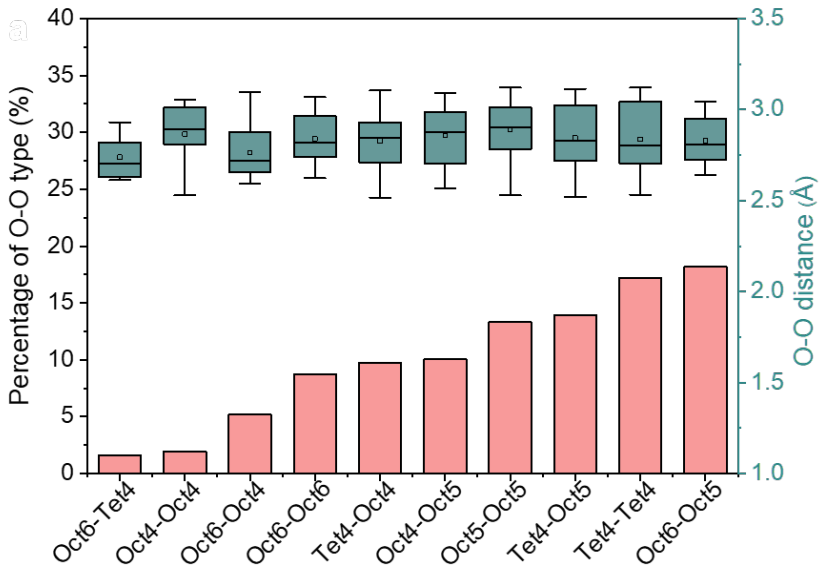

Fig. S7 O-O type distribution and O-O bond length statistics in $Li_{1.7}Mn_{1.6}O_{3.7}F_{0.3}$.

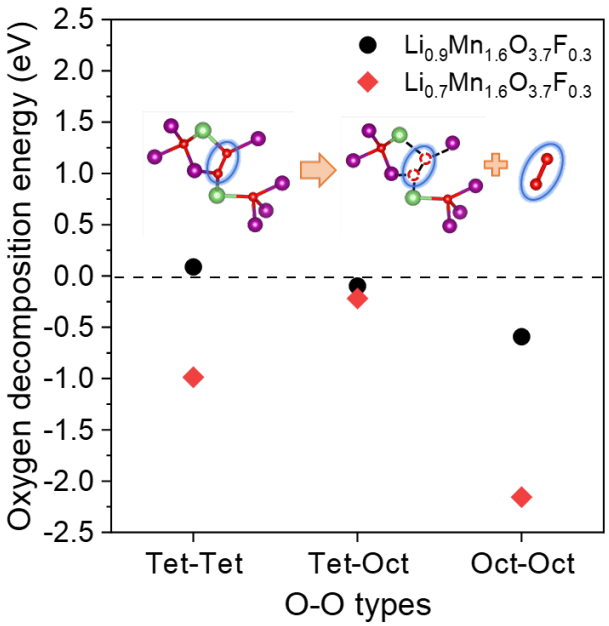

Fig. S8 Oxygen decomposition energy of different O-O types in $Li_{0.9}Mn_{1.6}O_{3.7}F_{0.3}$ and $Li_{0.7}Mn_{1.6}O_{3.7}F_{0.3}$. Tet-Tet is the abbreviation of O(Tet-4)-O(Tet-4), Tet-Oct is O(Tet-4)-O(Oct-5), Oct-Oct is short for O(Oct-4)-O(Oct-6). The upper inset of the diagram shows a schematic illustration of the oxygen molecule escape from the structure.

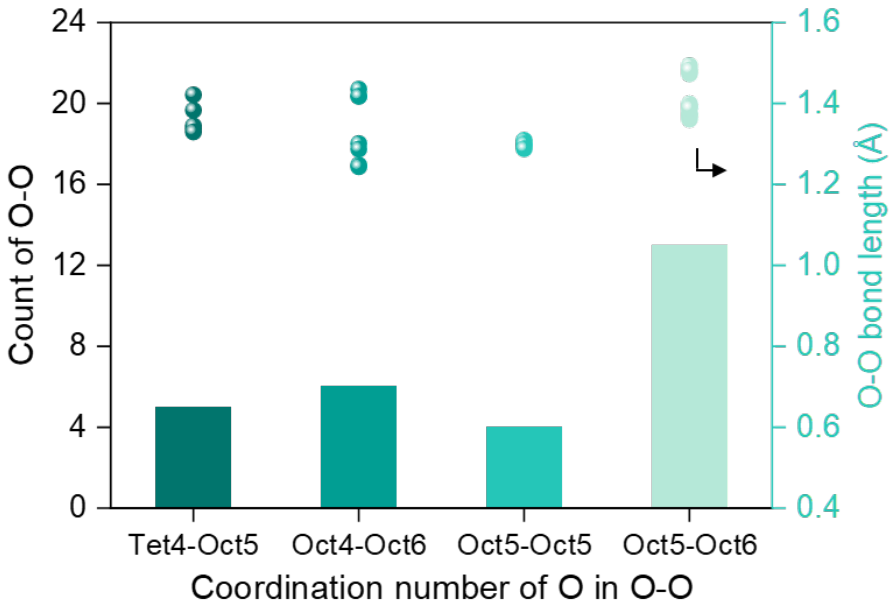

Fig. S9 Statistics of O-O types and bond lengths obtained from metadynamics structures. Note: Tet4-Oct5 is an abbreviation for O(Tet-4)-O(Oct-5).

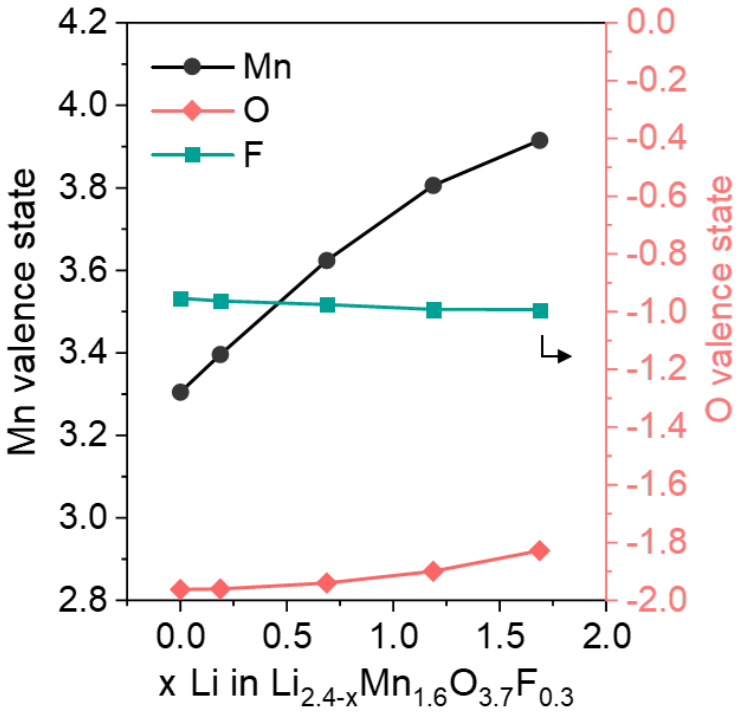

Fig. S10 The valence states of Mn, O, and F in $Li_{2.4-x}Mn_{1.6}O_{3.7}F_{0.3}$ (x=0, 0.2, 0.7, 1.2, 1.7) are determined from the average magnetic moment.

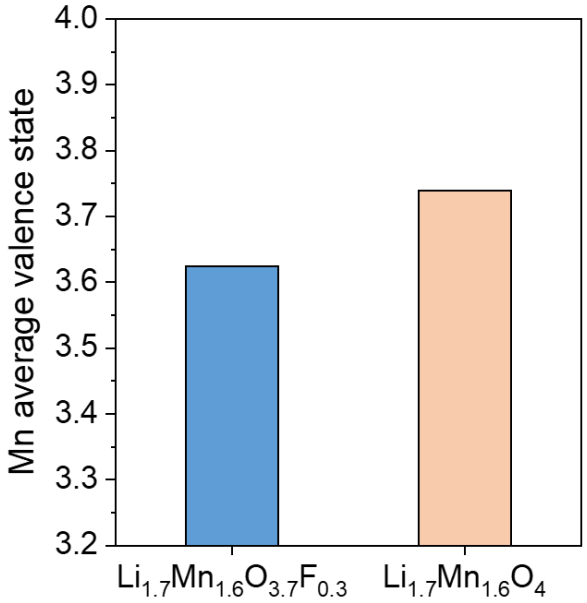

Fig. S11 The average valence of Mn in $Li_{1.7}Mn_{1.6}O_{3.7}F_{0.3}$ and $Li_{1.7}Mn_{1.6}O_4$ are determined from the average magnetic moment.

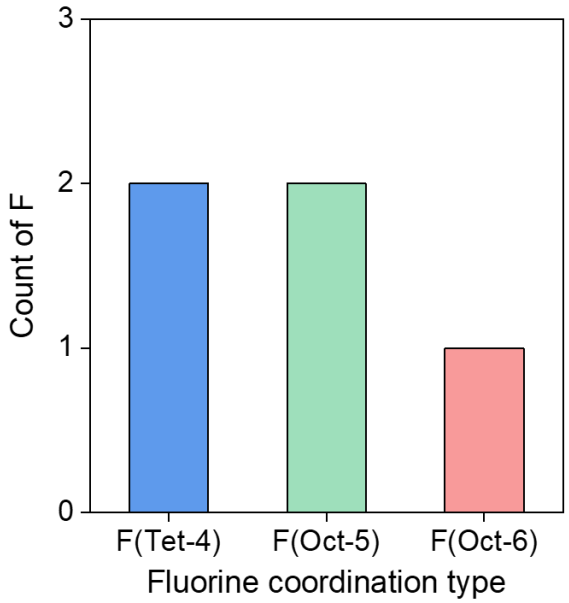

Fig. S12 The number of the three types of fluorine coordination configurations in $Li_{1.7}Mn_{1.6}O_{3.7}F_{0.3}$.

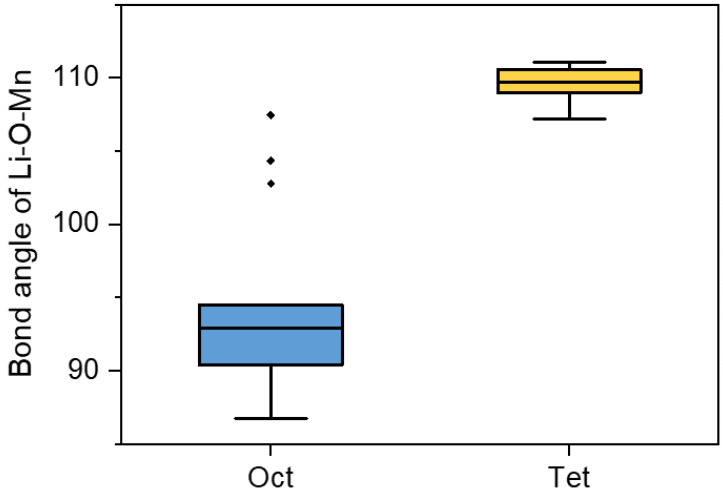

Fig. S13 Li-O-Mn bond angle distribution in the $Li_{1.7}Mn_{1.6}O_{3.7}F_{0.3}$, where Oct contains Oct-4, Oct-5, Oct-6 configurations.

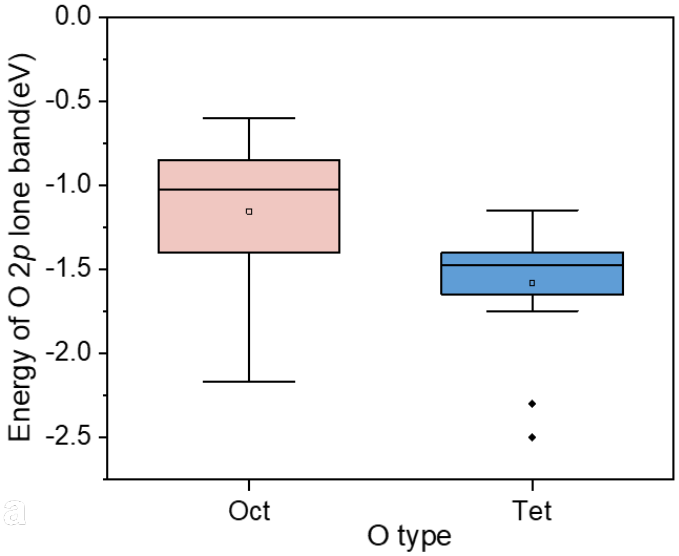

Fig. S14 Energy level distribution of the O 2*p* lone band in the O(Oct) and O(Tet) configurations.

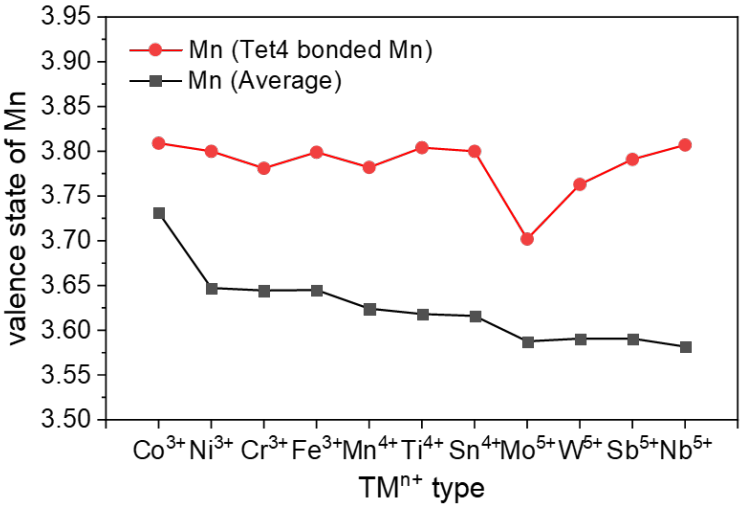

Fig. S15 The valence state of tetrahedral center Mn and the average valence state of Mn in the structure of $Li_{1.7}Mn_{1.6-x}TM_xO_{3.7}F_{0.3}$ (x=0.0625) are obtained by magnetic moment.

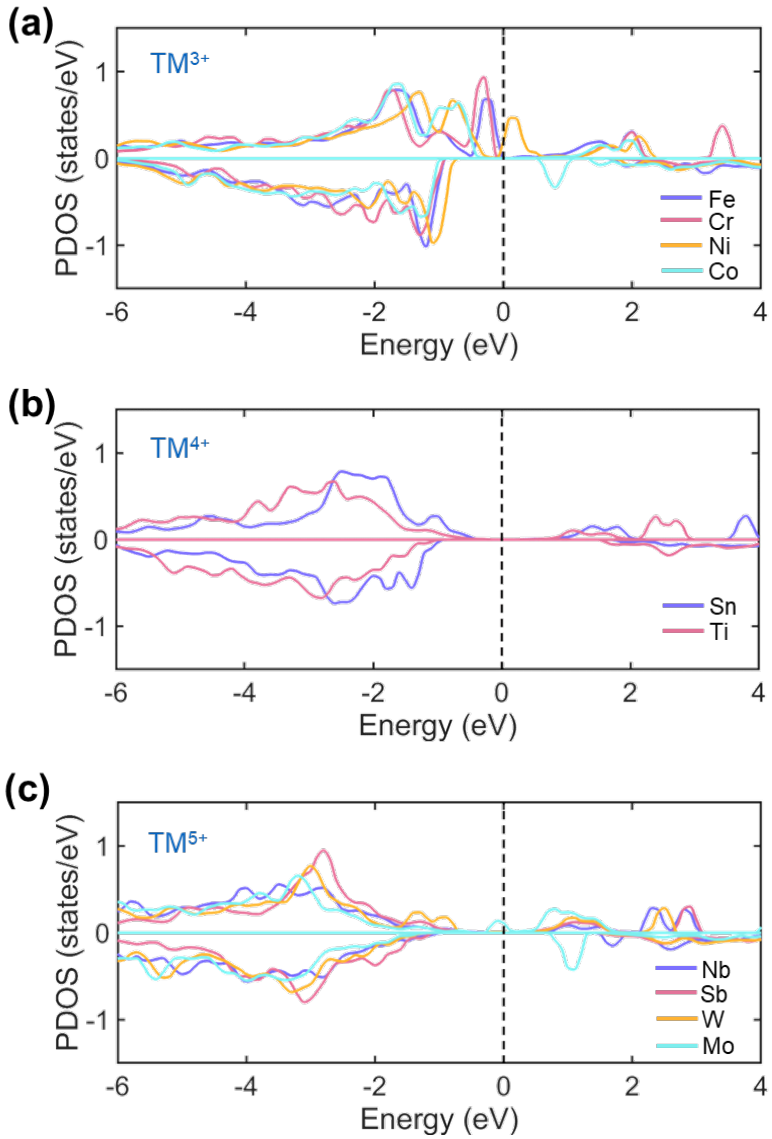

Fig. S16 Electronic structural characterization of TM-substituted tetrahedral oxygen. (a) Trivalent TM: Fe^{3+}, Cr^{3+}, Ni^{3+}, Co^{3+}. (b) Tetravalent TM substitution: Sn^{4+}, Ti^{4+}. (c) Pentavalent TM substitution: Nb^{5+}, Sb^{5+}, W^{5+}, Mo^{5+}.

Supplementary Tables

Table S1. Total and relative energies of calculated 6 low-energy structures of $Li_{2.4}Mn_{1.6}O_{3.7}F_{0.3}$.

Configuration of $Li_{2.4}Mn_{1.6}O_{3.7}F_{0.3}$	Total energy (eV/atom)	Relative energy(eV/atom)
S_1	-6.2519	0.0000
S_2	-6.2163	0.0059
S_3	-6.2335	0.0173
S_4	-6.2142	0.0204
S_5	-6.2372	0.0277
S_6	-6.2216	0.0457

Table S2. Total and relative energies of calculated 6 low-energy structures of $Li_{2.2}Mn_{1.6}O_{3.7}F_{0.3}$.

Configuration of $Li_{2.2}Mn_{1.6}O_{3.7}F_{0.3}$	Total energy (eV/atom)	Relative energy(eV/atom)
S_1	-6.3165	0.0000
S_2	-6.3141	0.0025
S_3	-6.3065	0.0100
S_4	-6.3008	0.0158
S_5	-6.3006	0.0160
S_6	-6.2914	0.0252

Table S3. Total and relative energies of calculated 6 low-energy structures of $Li_{1.9}Mn_{1.6}O_{3.7}F_{0.3}$.

Configuration of $Li_{1.9}Mn_{1.6}O_{3.7}F_{0.3}$	Total energy (eV/atom)	Relative energy(eV/atom)
S_1	-6.3593	0.0000
S_2	-6.3537	0.0057
S_3	-6.3496	0.0097
S_4	-6.3439	0.0154
S_5	-6.3438	0.0156
S_6	-6.3410	0.0183

Table S4. Total and relative energies of calculated 6 low-energy structures of $Li_{1.7}Mn_{1.6}O_{3.7}F_{0.3}$.

Configuration of $Li_{1.7}Mn_{1.6}O_{3.7}F_{0.3}$	Total energy (eV/atom)	Relative energy(eV/atom)
S_1	-6.3860	0.0000
S_2	-6.3857	0.0004
S_3	-6.3800	0.0060
S_4	-6.3760	0.0100
S_5	-6.3750	0.0111
S_6	-6.3705	0.0155

Table S5. Total and relative energies of calculated 6 low-energy structures of $Li_{1.4}Mn_{1.6}O_{3.7}F_{0.3}$.

Configuration of $Li_{1.4}Mn_{1.6}O_{3.7}F_{0.3}$	Total energy (eV/atom)	Relative energy(eV/atom)
S_1	-6.4161	0.0000
S_2	-6.4117	0.0044
S_3	-6.3982	0.0179
S_4	-6.3896	0.0265
S_5	-6.3870	0.0291
S_6	-6.3810	0.0351

Table S6. Total and relative energies of calculated 6 low-energy structures of $Li_{1.2}Mn_{1.6}O_{3.7}F_{0.3}$.

Configuration of $Li_{1.2}Mn_{1.6}O_{3.7}F_{0.3}$	Total energy (eV/atom)	Relative energy(eV/atom)
S_1	-6.4324	0.0000
S_2	-6.4215	0.0109
S_3	-6.4069	0.0255
S_4	-6.3988	0.0337
S_5	-6.3957	0.0367
S_6	-6.3814	0.0510

Table S7. Total and relative energies of calculated 6 low-energy structures of $Li_{0.9}Mn_{1.6}O_{3.7}F_{0.3}$.

Configuration of $Li_{0.9}Mn_{1.6}O_{3.7}F_{0.3}$	Total energy (eV/atom)	Relative energy(eV/atom)
S_1	-6.4431	0.0000
S_2	-6.4236	0.0195
S_3	-6.4109	0.0322
S_4	-6.4094	0.0337
S_5	-6.3971	0.0460
S_6	-6.3756	0.0675

Table S8. Total and relative energies of calculated 6 low-energy structures of $Li_{0.7}Mn_{1.6}O_{3.7}F_{0.3}$.

Configuration of $Li_{0.7}Mn_{1.6}O_{3.7}F_{0.3}$	Total energy (eV/atom)	Relative energy(eV/atom)
S_1	-6.4617	0.0000
S_2	-6.4496	0.0121
S_3	-6.4411	0.0206
S_4	-6.4352	0.0265
S_5	-6.4231	0.0386
S_6	-6.4083	0.0534

Table S9. Lattice parameters and the shortest O-O bond length of the global minimum structures.

Type	a (Å)	b (Å)	c (Å)	O-O bond length (Å)
$Li_{2.4}Mn_{1.6}O_{3.7}F_{0.3}$	8.22	16.78	8.15	2.59
$Li_{2.2}Mn_{1.6}O_{3.7}F_{0.3}$	8.20	16.50	8.19	2.52
$Li_{1.9}Mn_{1.6}O_{3.7}F_{0.3}$	8.14	16.40	8.17	2.51
$Li_{1.7}Mn_{1.6}O_{3.7}F_{0.3}$	8.05	16.49	8.25	2.50
$Li_{1.4}Mn_{1.6}O_{3.7}F_{0.3}$	8.18	16.06	8.22	2.51
$Li_{1.2}Mn_{1.6}O_{3.7}F_{0.3}$	8.22	15.88	8.13	2.50
$Li_{0.9}Mn_{1.6}O_{3.7}F_{0.3}$	8.26	15.77	8.06	2.44
$Li_{0.7}Mn_{1.6}O_{3.7}F_{0.3}$	8.49	13.75	8.44	1.29